applied sciences

MDPI

Communication

Fatigue Testing of Human Flexor Tendons Using a Customized 3D-Printed Clamping System

Mario Scholze [1,2,*], Sarah Safavi [3,4], Maziar Ramezani [5], Benjamin Ondruschka [6] and Niels Hammer [2,7,8,*]

1 Institute of Materials Science and Engineering, Chemnitz University of Technology, 09111 Chemnitz, Germany
2 Division of Macroscopic and Clinical Anatomy, Gottfried Schatz Research Center, Medical University of Graz, 8036 Graz, Austria
3 Department of Anatomy, University of Otago, Dunedin 9016, New Zealand
4 Department of Biomedical Engineering, Faculty of Engineering and Information Technology, The University of Melbourne, Melbourne, VIC 3010, Australia
5 Department of Mechanical Engineering, Auckland University of Technology, Auckland 1010, New Zealand
6 Institute of Legal Medicine, University Medical Center Hamburg-Eppendorf, 22529 Hamburg, Germany
7 Department of Orthopedic and Trauma Surgery, University of Leipzig, 04109 Leipzig, Germany
8 Fraunhofer IWU, Medical Branch, 01187 Dresden, Germany
* Correspondence: mario.scholze@mb.tu-chemnitz.de (M.S.); niels.hammer@medunigraz.at (N.H.); Tel.: +43-316-385-71100 (N.H.)

Featured Application: This novel 3D-printed clamping design allows for time efficient and seamless cyclic testing of biological soft tissues to obtain fatigue curves without the need for processing.

Abstract: Improved surgical procedures and implant developments for ligament or tendon repair require an in-depth understanding of tissue load-deformation and fatigue properties. Cyclic testing will provide crucial information on the behavior of these materials under reoccurring loads and on fatigue strength. Sparse data are available describing soft tissue behavior under cyclic loading. To examine fatigue strength, a new technology was trialed deploying 3D-printing to facilitate and standardize cyclic tests aiming to determine tendon fatigue behavior. Cadaveric flexor digitorum tendons were harvested and mounted for tensile testing with no tapering being made, using 3D-printed clamps and holder arms, while ensuring a consistent testing length. Loads ranging between 200 to 510 N were applied at a frequency of 4 Hz, and cycles to failure ranged between 8 and >260,000. S–N curves (Woehler curves) were generated based on the peak stresses and cycles to failure. Power regression yielded a combined coefficient of determination of stress and cycles to failure of $R^2 = 0.65$, while the individual coefficients for tissues of single donors ranged between $R^2 = 0.54$ and $R^2 = 0.88$. The here-presented results demonstrate that S–N curves of human tendons can be obtained using a standardized setting deploying 3D-printing technology.

Keywords: 3D (three-dimensional)-printing technology; fatigue life; high cycle fatigue tests; ligament; soft tissue mechanics; tendon biomechanics; S–N test; Woehler curve

Citation: Scholze, M.; Safavi, S.; Ramezani, M.; Ondruschka, B.; Hammer, N. Fatigue Testing of Human Flexor Tendons Using a Customized 3D-Printed Clamping System. *Appl. Sci.* **2022**, *12*, 7836. https://doi.org/10.3390/app12157836

Academic Editor: Claudio Belvedere

Received: 25 June 2022
Accepted: 26 July 2022
Published: 4 August 2022

1. Introduction

An estimate of 20 to 33% of the population worldwide is affected by musculoskeletal diseases, which are often related to ligament and tendon pathology [1–3]. Ligaments and tendons are dominated by extracellular matrix-rich collagenous structures with slow tissue metabolism and repair [4]. Therefore, facilitating tissue recovery and functionality within a reasonable time-frame following injury often requires surgery. To improve both the outcomes with surgical procedures and implants involving ligaments or tendons, it is vital to understand in depth their biomechanical behavior even in an intact state. Cyclic testing of biological materials may give fundamental information on the fatigue life and mechanisms that ultimately result in material failure [5]. The findings derived from fatigue

tests can be further objectified by so-called S–N curves (Woehler curves), indicating a function of cyclic stress and the number of cycles to failure.

S–N curves are commonplace in materials science of inanimate matter. In life science and especially in the biomechanics of soft tissues, however, fatigue testing of human tissues has so far only been conducted by a few groups resulting in accurate S–N curves [6–9]. Due to the natural characteristics of biological soft tissues resulting in transverse contraction, clamping forms a major issue [7,10,11]. Even in static testing scenarios or in low-cycle tests only entailing a few hundreds of cycles or less, continued slippage may result in premature failure at the clamping interface or in a complete slip out of the sample from the clamping. Considering that biological samples are built to withstand tens of thousands of cycles under versatile conditions, standard clamping techniques [7,12,13] are deemed unsuitable for cyclic conditions ex vivo.

Our group recently introduced a novel clamping technique using 3D-printing technology [14,15]. The modular and adaptable design allows soft tissue testing to be facilitated and standardized, overcoming limitations of conventional clamping methods. Similar approaches have now been adapted by others for quasi-static testing procedures [16]. This methods-focused report builds upon recent developments in 3D-printed clamping [14,15], modifying these techniques to provide standardized mounting options to assess tendon fatigue behavior based on cyclic testing. A secondary aim of this approach was to generate Woehler (S–N) curves from human flexor tendons ex vivo.

The aim was to establish a method to allow for cyclic fatigue testing of biological tissues, minimizing slippage, and thereby generating valuable data for material models under dynamic conditions. It was hypothesized that using a new 3D-printed design, S–N curves of flexor tendons can be generated reflecting a moderate ($R^2 \geq 0.5$) force–cycle relationship.

2. Materials and Methods

Human flexor tendons of the forearm and hand (flexor digitorum profundus and superficialis) were harvested bilaterally from cadavers from the Department of Anatomy, University of Otago, New Zealand, in a Crosado-embalmed condition [17]. Ethical approval was obtained from the University of Otago Ethics Committee (H17/20). The tissues were retrieved from the central part of the tendons, i.e., areas remote from the origin of insertion sites and also distant from the transition between muscle fibers and tendon. The tendons were sectioned perpendicular to the main fiber direction in a condition without applying prestrain and then freed from surrounding tissues. Following tissue retrieval, the tissues were stored in sealed plastic bags filled with 1.3volume% phenoxyethanol under light exclusion conditions. Immediately prior to the tests, the tendons were rinsed with isotonic (9 g/L NaCl) saline for 24 hours to remove the reversible effects of the ethanol embalming related to the denaturation of the extracellular matrix tertiary structures before the fatigue tests began [13]. All manipulations of the tendons were carried out in a moist environment to minimize drying [18]. Fifty samples from six different human donors were tested at 20 °C under ambient room conditions. Seven samples were only used for the combined analysis, as the number of samples per donor was too low for subject-dependent analysis ($n < 6$).

The tendons were mounted individually in two 3D-printed clamps printed of commercial type polylactic acid (PLA) using an Ultimaker 3 Extended printer (Ultimaker B.V., Geldermalsen, The Netherlands). One clamp was used for each side. Deviating from previous interlocking two-part designs [18–21], this new setup involved a single squeezing part with a central opening. The clamps consisted of a pattern of small 4-sided pyramids (design with flat pyramids, pyramid height = 0.75 mm, diagonal base = 2.12 mm). The pyramid patterns of the opposing sides interlock during clamping and thus create an additional form fit. Further details on the clamps and the setup can be found elsewhere [14,15]. The inner aspect of the clamp was designed to have flattened pyramid structures, customized for the cyclic tensile testing. Holder arms that can be attached to the clamps ensure a

consistent clamping length and facilitate the mounting. Figure 1 shows the described parts assembled.

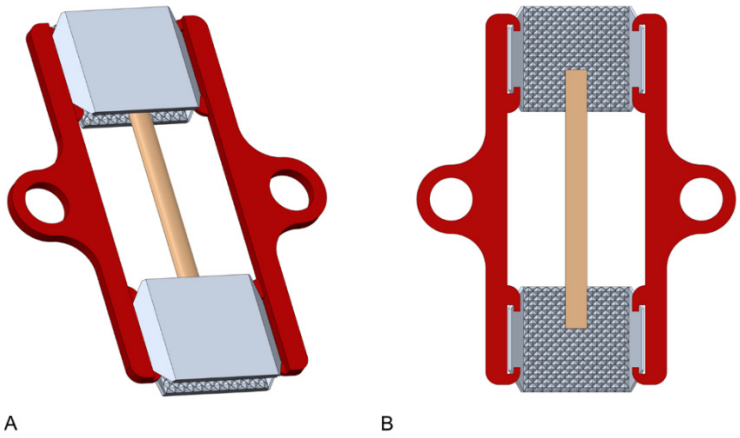

Figure 1. Computer-aided design model of the assembled clamps and holder arms (including the schematic representation of a sample). (**A**) 3D view, (**B**) cross-sectional view.

For the mechanical tests, an MTS Landmark Model 370.02 Servo Hydraulic Test System (MTS Systems Corporation, Eden Prairie, MN, USA) with a maximum applicable load of 25 kN and a standard load cell was used under cyclic tensile fatigue loading. Before the cyclic loading began, the axial displacement of the machine was set to 0 mm. The tissue clamping distance was standardized to 40 mm, and a parallel alignment of the tissues within the clamps as well as between the two clamps for each specimen was ensured. To this end, 3D-printed holder arms of thermoplastic polyurethane (TPU) were attached to the clamps as shown in Figure 2A. The clamps were then placed in the machine's jaws, and the pressure of the surrounding hydraulic clamps was standardized to 6 MPa (Figure 2B).

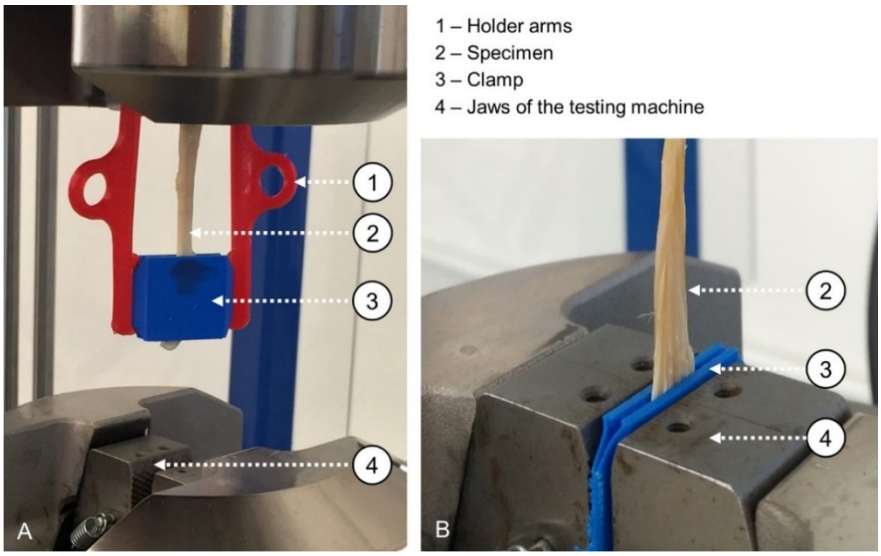

Figure 2. Specimen mounting in the testing machine (**A**) using clamps on each side and flexible holder arms to facilitate accurate placement with a consistent testing length and (**B**) setup ready for mechanical testing with 3D-printed clamps and a clamped tendon placed between the closed external jaws.

Prior to the fatigue testing, an axial pre-load of 10 N on the specimen allowed for stabilized conditions to determine the cross-section area. A digital caliper (Mitutoyo Corporation, Sakado, Kawasaki, Kanagawa, Japan; accuracy ± 0.02 mm) was used to measure the tendons' widths and thicknesses. These measures were obtained from three

areas of the tendon at the bottom, central, and top aspect of the tendon and then averaged to consider the irregular shape of the tendon along its fiber direction. The machine was then set to a cyclic loading protocol with a minimum load of 10 N and a maximum load ranging between 200 and 510 N at a frequency of 4 Hz. These values were chosen according to loads observed in tensile tests carried out on human forearm tendons in a previous study [22]. To minimize the risk of specimen failure occurring in the first cycles, stresses lower than reported tendons' ultimate tensile strengths were chosen (pilot test). The loads were increased stepwise for each sample of a group to obtain the number of cycles for a range of stresses. The starting load was set to 10 N and increased by 20 N each step up to the maximum load range of 200–510 N. The loads were constantly monitored for the full duration of the experiments, and the samples were constantly moistened at 15-minute intervals by spraying isotonic 0.9mass% saline onto the tissue surface. From the obtained data, Woehler curves were generated. A power regression according to Equation (1) was performed using Excel 16.0.15330 (Microsoft Corporation, Redmond, WA, USA), and the coefficient of determination R^2 was calculated by including x_i (cycles to failure) and y_i (peak stresses) for subject-dependent and combined values, as well as the respective number of correlated values n. The corresponding parameters a and b were determined using Equations (2) and (3). Individual coefficients R^2 were calculated as seen in Equation (4).

$$y = ax^b \tag{1}$$

$$b = \frac{\sum \ln x_i \ln y_i - n\frac{\sum \ln x_i}{n}\frac{\sum \ln y_i}{n}}{\sum \ln x_i^2 - n\left(\frac{\sum \ln x_i}{n}\right)^2} \tag{2}$$

$$a = exp\left(\frac{\sum lny_i}{n} - b\frac{\sum lnx_i}{n}\right) \tag{3}$$

$$R^2 = \frac{\sum \ln x_i \ln y_i - n\frac{\sum \ln x_i}{n}\frac{\sum \ln y_i}{n}}{\sqrt{\sum \ln x_i^2 - n\left(\frac{\sum \ln x_i}{n}\right)^2}\sqrt{\sum \ln y_i^2 - n\left(\frac{\sum \ln y_i}{n}\right)^2}} \tag{4}$$

3. Results

Cyclic tests were conducted and evaluated for all tendons, and S–N curves were computed for individual cadavers and combined overall. The set loads for the tests and the cross-sectional areas were used to calculate the stresses within the tendons. Forces ranged between 200 and 510 N, and the number of cycles between 8 and >260,000. Mean values and standard deviations of specimen average cross-sectional areas; and minimum and maximum values of the axial forces, stress, and cycles-to-failure for each group and pooled data are summarized in Table 1.

Integrating the number of cycles until failure under different peak stress levels, fatigue diagrams were calculated. Figure 3 exemplifies the subject-dependent S–N curves, which combine the results for the samples from each donor. The number of cycles is displayed on the x-axis with a logarithmic scale, and the peak stresses on the y-axis with a linear scale. All three curves yielded a clear tendency towards decreasing stress values for higher numbers of cycles. Individual R^2 ranged between 0.54 and 0.88. None of the individual S–N curves yielded R^2 values below 0.5. The Woehler curve for the combined results of all tendons can be seen in Figure 4. The R^2 for the combined data was 0.65. Material failure was observed in the clamping area for all samples. Failure of the clamps was observed in some of the samples following the mounting. In addition, 38% of the clamps used showed failure patterns after the test, which occurred either during initial clamping or due to cyclic loading of the printed structures. There were four different types of failure—transverse and longitudinal, each either occurring in the middle or the edge of the clamp. Most failures were observed on the edges of the clamps. Out of these failures, 78.3% were longitudinal and 21.7% transverse. Only 0.6% of the clamps failed longitudinally in the central area.

Table 1. Test results of the sample groups' individual cadavers and combined mean values and standard deviations of the cross-sectional areas, minimum and maximum values of peak axial forces, peak stresses and number of cycles until failure, and coefficient of determination of Woehler curves obtained through power regression. * Individual values of two donors are not given due to a sample size of less than six.

Tissue ID	0813-5 (n = 11)	0814-4 (n = 9)	0801-4 (n = 11)	0822-4 (n = 12)	Combined (n = 50 *)
Cross-sectional area (mm^2)	13.42 ± 4.21	9.85 ± 2.09	11.16 ± 4.72	13.22 ± 4.69	12.04 ± 4.40
Peak axial force (N) (min–max)	250–510	250–500	200–500	240–500	200–510
Peak stress (MPa) (min–max)	17.08–49.59	22.31–79.79	10.45–88.86	11.99–64.66	10.45–88.86
Number of cycles (min–max)	16–24,364	8–11,744	16–261,784	32–10,476	8–261,784
Coefficient of determination R^2	0.84	0.68	0.88	0.54	0.65

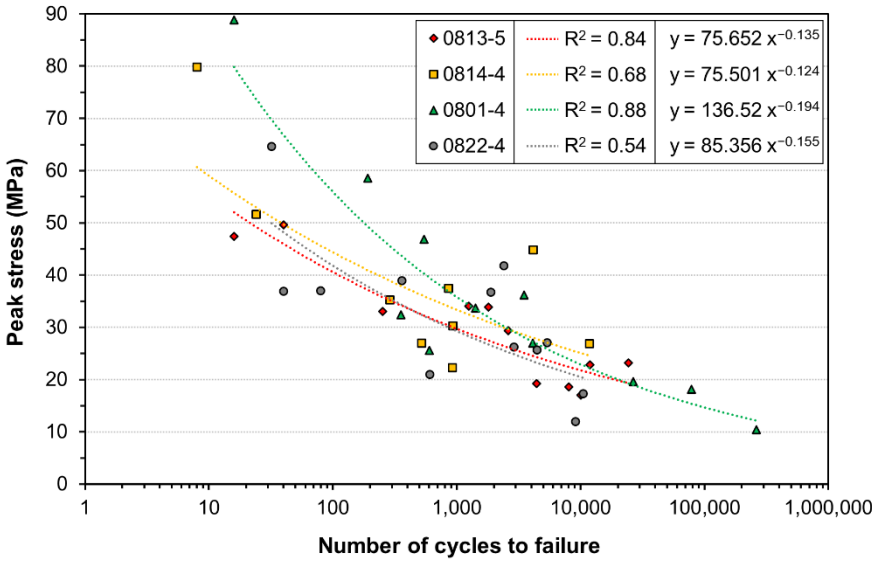

Figure 3. Subject-dependent S–N curves for tissues obtained from four donor cadavers. Each graph is approximated from the obtained data points using power regression.

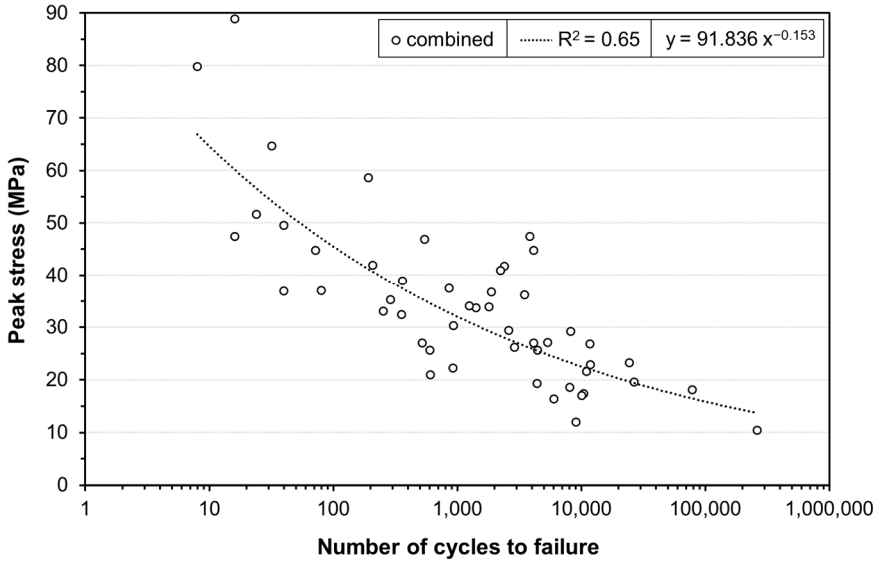

Figure 4. Combined S–N curve for all tendon samples. Approximated graph from the data points using power regression.

4. Discussion

Experimental data from six individual donors, ranging from two to twelve samples each, were evaluated to generate S–N (Woehler) curves. Although scattering of the data points was observed for all groups, coefficients of determination between 0.54 and 0.88 were achieved with a combined R^2 of 0.65. In a previous study, Wren et al. used 25 Achilles tendons for cyclic testing, resulting in an S–N curve with R^2 = 0.34 [8]. The scattering of the individual data points in this and other studies may likely be related due to natural inconsistencies of human tendons. The individual measurements of the tendon samples highly vary, even within the same individuals, due to their natural geometry. Moreover, the state of the tissue is dependent on the donor's age, sex, and health status. The preservation method and water content following the harvesting of the sample also bias the results [18,23].

A variety of approaches to specimen clamping has been deployed to date. Methods that hold fibers of the outer layers only, including gluing or cryogenic clamping, commonly result in altered testing strength and stiffness [10]. Ker et al. air-dried the ends of the specimens to be clamped instead, while keeping the remaining parts of the same sample moist to reduce the tissues' thickness and flexibility in the clamping area [10]. While this technique may facilitate the clamping, it also causes stress concentrations at the transition area between the dry and the moist parts [10,24]. Selecting another approach, Fung et al. used sandpaper-covered plates for fatigue testing of rat tendons [25]. This technique seems rather unsuitable for fatigue testing of human samples, as marked slippage was observed with relevant impacts on the accuracy of the results [15]. Equally, cryogenic clamps have been applied in studies [12]. This being a time-consuming mounting technology, the low temperatures also result in altered tissue properties and facilitate intrinsic specimen failure at the transition areas, where tissue changes from frozen to unfrozen parts. Shi et al. introduced a new design of titanium clamps with lateral block boards and asymmetrical teeth jaws that does not require the samples to be frozen. However, due to the stress caused by the clamps, sample failure was predominantly observed in the clamping area and not in the intended central section, indicating significant influence of the clamps used [26]. A method called partial plastination was introduced by Steinke et al., aiming at minimizing the occurring measurement errors due to material slippage without involving such freezing-related issues [13,27]. This dehydrates and impregnates the tissues' ends with resin, forming a flat and non-contractile surface to enhance mounting stability [13,27]. Sichting et al. quantified the material slippage occurring even in partially plastinated

samples and found resulting measurement errors of up to 18%, indicating the need for digital image correlation [28]. As a consequence, fatigue testing is hampered by the existing clamping techniques.

The new method presented here allows immediate testing of the sample without changing the tissue state by decreasing temperature, exposing it to chemicals and leading to denaturation, dehydration, or degreasing it or creating a sharp interface, with influence on the mechanical behavior. This may allow for more realistic in vitro tests of engineered tissues, e.g., following acellularization or chemical treatment, thus allowing conclusions to be derived on their durability before cellular ingrowth and remodeling occurs [19,29–32]. The internal pyramid structure of the here-presented clamps allows testing without chemical alterations while simultaneously reducing slippage. Scholze et al. introduced different sharp- and smooth-edged pyramid designs for tissues of different thicknesses [14,15]. External damage to the tissue in the clamping areas was reduced when compared to conventional clamping by metal jaws. Such findings have already been quantified in another study by our group [15]. Moreover, the handling and insertion into the testing device was simplified due to the modular setup, resulting in a time advantage when handling the tissues. The time required for specimen preparation, mounting, and testing was not bound to the additional time needed for hardening of the embedding material, such as epoxy resin, which was used in a previous study [13,28]. The clamp-to-clamp length is predefined by the holder arms and therefore standardized for every test carried out. In addition, the alignment and tested region of the samples is exactly defined before the insertion and does not require manual adjustment in the testing machine. An occurrence of improper sample alignment during clamping or sample damage (e.g., by the jaws) during insertion was not observed when using the 3D-printed system. All of the given adjustments of the clamping and mounting devices were made in favor of providing a standardized, time efficient, and easy-to-handle design, resulting in the first successful attempt to obtain fatigue curves of human tendon samples while at the same time minimizing material slippage to achieve $>10^5$ loading cycles ex vivo.

In addition to their ease of use, all parts of the clamps and mounts are highly accessible and easy to adapt. The design of the clamps and holder arms can be customized to suit various soft tissues of different dimensions and lengths. Another advantage when using 3D-printing technology is the freedom to choose the most suited printing material. PLA used in this study is a commonly used and accessible filament printing material and is biodegradable [33]. Therefore, depending on the material chosen, 3D-printing technology allows for the reduction of non-degradable waste in biomechanical testing. Due to a lack of reliable and standardized methodical cyclic testing of soft tissues, no data are available to date to predict tissue behavior under cyclic loading; 3D-printing technology provides accessibility, ease of use, and adjustability, as well as sustainability and may therefore be the infrastructure for the future assessment of soft tissues. This standardized method may provide the opportunity to learn more about the mechanics of tissue. The design of the presented clamps is optimized for less compressive biological samples with a thicker cross-sectional area and may be used for various types of biomechanical testing. There are various factors influencing the mechanical behavior of soft tissues, which to date have not been fully quantified. The load-deformation characteristics of tendons, ligaments, and other soft tissues are individual and may change with age, injury or disease, and other factors. Facilitating and standardizing the assessment of these materials may enable us to better understand the story behind the tissue—how it influences its mechanical behavior and quantifies its mechanical age. Gaining a better understanding of how tissues change may provide valuable information for the optimization of treatments to avoid injuries or improve surgical treatments and rehabilitation after injury. Further, the here-given setup may allow for assessing tendon (fatigue) damage at substructural levels, elucidating site-different mechanical behavior of tendon structures [34].

Limitations

The mechanical testing of the samples was carried out ex vivo outside of wet chambers and at room conditions. This setup comes with a number of limitations, shortening the life span of the tissues, as the mechanical properties differ from those of living tissue. As a consequence, the missing tissue surrounding the tendons in the center may have resulted in diminished hydration effects. Despite moistening of the samples prior to the testing and maintaining a moist environment, drying effects may occur. The water content of the tissue may vary throughout the preparation and testing process. To keep the natural fiber orientation intact without creating a likely failure site, the tendon specimens were left intact. This as a result led to unintended failure sites but was necessary to allow for fatigue testing without premature failure. The main failure site observed was in the clamping area, potentially due to shearing or squeezing of the sample considering the sample to be uniformly thick. This needs to be considered in future studies. The natural tapering of the tendons was randomly assigned to the rigid and moving clamping side, which may have influenced the results. The cross-sectional area was calculated by assuming a rectangular shape and averaging three areas of the tendons, which moreover influenced the calculation of the peak stresses. In future studies, the smallest cross-sectional areas could, for example, be detected and measured by optical methods. During the testing, 38% of the 3D-printed clamps failed, mainly on the edge areas. As this can potentially influence the results by acting as a stress concentrator and lead to lower tolerable maximum forces of such tissues, further analyses to quantify these effects, e.g., using image correlation techniques, is recommended for future studies. While failure on the edges of the clamps was assessed as not having a major effect on the results, it does preclude them from being reused for further testing. Optimizing the design and/or using other materials than PLA for the manufacturing of the clamps could enable multiple use as well as reduced damage of the clamps and therefore reduced material costs.

5. Conclusions

A new custom-built design of 3D-printed clamps was utilized and trialed to obtain biomechanical data of human tendons under cyclic loading and to generate S–N curves. In pilot tests with sandpaper and metal clamps, cyclic testing of the tendons was not possible and resulted in a high number of direct failures of the tendons in the clamping area or excessive specimen slippage. The use of clamps with pyramidal structures has already been successfully applied to quasi-static tests [14,15] and was successfully applied to cyclic testing of non-tapered tendons in their natural shapes in this study. Using the here-presented 3D-printed clamps and holder arms vastly facilitated the preparation and mounting of the samples when compared to the other clamping methods. As a consequence, our hypothesis that S–N curves based on fatigue tests using the new 3D-printed design provide moderate accuracy ($R^2 \geq 0.5$) can be accepted. The here-presented method can be used to gain more in-depth knowledge of biomechanical properties of ligaments and tendons under cyclic loading to help understand mechanisms of load transfer and failure, and possibly to provide knowledge about optimized surgical treatment of soft tissue reconstruction.

Author Contributions: Conceptualization, M.S., M.R., B.O. and N.H.; methodology, M.S. and M.R.; validation, B.O. and N.H.; writing—original draft preparation, M.S., S.S. and N.H.; writing—review and editing, M.R., B.O. and N.H.; supervision, N.H. All authors have read and agreed to the published version of the manuscript.

Funding: Publication of this article was funded by Chemnitz University of Technology.

Institutional Review Board Statement: The Ethics Committee of the University of Otago, New Zealand, gave ethical approval for conducting these experiments (H17/20).

Informed Consent Statement: Informed consent was obtained from all subjects involved in the study for their bodies to be used in research as stipulated by the 2008 Human Tissue Act of New Zealand.

Data Availability Statement: Data are made available upon reasonable request by the corresponding authors.

Acknowledgments: The authors would like to thank the body donors for bequeathing their post mortem tissues for research purposes. We would also like to thank Corentin Rouquette, Jean-Baptiste Le Joncour, and Marcel Schäfer for their contributions to the experiments.

Conflicts of Interest: The authors declare no conflict of interest.

References

1. Barber, F.A.; Aziz-Jacobo, J. Biomechanical testing of commercially available soft-tissue augmentation materials. *Arthroscopy* **2009**, *25*, 1233–1239. [CrossRef] [PubMed]
2. Branch, J.P. A tendon graft weave using an acellular dermal matrix for repair of the Achilles tendon and other foot and ankle tendons. *J. Foot Ankle Surg.* **2011**, *50*, 257–265. [CrossRef] [PubMed]
3. Rubin, L.; Schweitzer, S. The use of acellular biologic tissue patches in foot and ankle surgery. *Clin. Podiatr. Med. Surg.* **2005**, *22*, 533–552. [CrossRef] [PubMed]
4. Ellison, M.E.; Duenwald-Kuehl, S.; Forrest, L.J.; Vanderby, R., Jr.; Brounts, S.H. Reproducibility and feasibility of acoustoelastography in the superficial digital flexor tendons of clinically normal horses. *Am. J. Vet. Res.* **2014**, *75*, 581–587. [CrossRef]
5. Bai, Y.; Jin, W.-L. Chapter 25—Fatigue Capacity. In *Marine Structural Design*, 2nd ed.; Butterworth-Heinemann: Oxford, UK, 2016; pp. 489–507. [CrossRef]
6. Martin, C.; Sun, W. Fatigue damage of collagenous tissues: Experiment, modeling and simulation studies. *J. Long Term Eff. Med. Implant.* **2015**, *25*, 55–73. [CrossRef]
7. Schechtman, H.; Bader, D.L. Fatigue damage of human tendons. *J. Biomech.* **2002**, *35*, 347–353. [CrossRef]
8. Wren, T.A.; Lindsey, D.P.; Beaupre, G.S.; Carter, D.R. Effects of creep and cyclic loading on the mechanical properties and failure of human Achilles tendons. *Ann. Biomed. Eng.* **2003**, *31*, 710–717. [CrossRef]
9. Schechtman, H.; Bader, D.L. In vitro fatigue of human tendons. *J. Biomech.* **1997**, *30*, 829–835. [CrossRef]
10. Ker, R.F.; Wang, X.T.; Pike, A.V. Fatigue quality of mammalian tendons. *J. Exp. Biol.* **2000**, *203*, 1317–1327. [CrossRef]
11. Shepherd, J.H.; Screen, H.R. Fatigue loading of tendon. *Int. J. Exp. Pathol.* **2013**, *94*, 260–270. [CrossRef]
12. Bowser, J.E.; Elder, S.H.; Rashmir-Raven, A.M.; Swiderski, C.E. A cryogenic clamping technique that facilitates ultimate tensile strength determinations in tendons and ligaments. *Vet. Comp. Orthop. Traumatol.* **2011**, *24*, 370–373. [CrossRef] [PubMed]
13. Steinke, H.; Lingslebe, U.; Bohme, J.; Slowik, V.; Shim, V.; Hadrich, C.; Hammer, N. Deformation behavior of the iliotibial tract under different states of fixation. *Med. Eng. Phys.* **2012**, *34*, 1221–1227. [CrossRef] [PubMed]
14. Scholze, M.; Safavi, S.; Li, K.C.; Ondruschka, B.; Werner, M.; Zwirner, J.; Hammer, N. Standardized tensile testing of soft tissue using a 3D printed clamping system. *HardwareX* **2020**, *8*, e00159. [CrossRef]
15. Scholze, M.; Singh, A.; Lozano, P.F.; Ondruschka, B.; Ramezani, M.; Werner, M.; Hammer, N. Utilization of 3D printing technology to facilitate and standardize soft tissue testing. *Sci Rep.* **2018**, *8*, 11340. [CrossRef] [PubMed]
16. Vella Wood, M.; Casha, A.; Gatt, A.; Formosa, C.; Chockalingam, N.; Grima, J.N.; Gatt, R. 3D Printed Clamps to Study the Mechanical Properties of Tendons at Low Strains. *Physica Status Solidi (B)* **2019**, *256*, 1800159. [CrossRef]
17. Crosado, B.; Loffler, S.; Ondruschka, B.; Zhang, M.; Zwirner, J.; Hammer, N. Phenoxyethanol-Based Embalming for Anatomy Teaching: An 18 Years' Experience with Crosado Embalming at the University of Otago in New Zealand. *Anat. Sci. Educ.* **2020**, *13*, 778–793. [CrossRef] [PubMed]
18. Lozano, P.F.; Scholze, M.; Babian, C.; Scheidt, H.; Vielmuth, F.; Waschke, J.; Ondruschka, B.; Hammer, N. Water-content related alterations in macro and micro scale tendon biomechanics. *Sci. Rep.* **2019**, *9*, 7887. [CrossRef]
19. Zwirner, J.; Ondruschka, B.; Scholze, M.; Schulze-Tanzil, G.; Hammer, N. Load-deformation characteristics of acellular human scalp: Assessing tissue grafts from a material testing perspective. *Sci. Rep.* **2020**, *10*, 19243. [CrossRef]
20. Zwirner, J.; Ondruschka, B.; Scholze, M.; Schulze-Tanzil, G.; Hammer, N. Biomechanical characterization of human temporal muscle fascia in uniaxial tensile tests for graft purposes in duraplasty. *Sci. Rep.* **2021**, *11*, 2127. [CrossRef] [PubMed]
21. Zwirner, J.; Scholze, M.; Waddell, J.N.; Ondruschka, B.; Hammer, N. Mechanical Properties of Human Dura Mater in Tension—An Analysis at an Age Range of 2 to 94 Years. *Sci. Rep.* **2019**, *9*, 16655. [CrossRef]
22. Weber, J.F.; Agur, A.M.; Fattah, A.Y.; Gordon, K.D.; Oliver, M.L. Tensile mechanical properties of human forearm tendons. *J. Hand Surg. Eur. Vol.* **2015**, *40*, 711–719. [CrossRef] [PubMed]
23. Schleifenbaum, S.; Prietzel, T.; Hadrich, C.; Mobius, R.; Sichting, F.; Hammer, N. Tensile properties of the hip joint ligaments are largely variable and age-dependent—An in-vitro analysis in an age range of 14–93 years. *J. Biomech.* **2016**, *49*, 3437–3443. [CrossRef]
24. Wang, X.T.; Ker, R.F.; Alexander, R.M. Fatigue rupture of wallaby tail tendons. *J. Exp. Biol.* **1995**, *198*, 847–852. [CrossRef] [PubMed]
25. Fung, D.T.; Wang, V.M.; Laudier, D.M.; Shine, J.H.; Basta-Pljakic, J.; Jepsen, K.J.; Schaffler, M.B.; Flatow, E.L. Subrupture tendon fatigue damage. *J. Orthop. Res.* **2009**, *27*, 264–273. [CrossRef] [PubMed]
26. Shi, D.; Wang, D.; Wang, C.; Liu, A. A novel, inexpensive and easy to use tendon clamp for in vitro biomechanical testing. *Med. Eng. Phys.* **2012**, *34*, 516–520. [CrossRef]

27. Hammer, N.; Lingslebe, U.; Aust, G.; Milani, T.L.; Hadrich, C.; Steinke, H. Ultimate stress and age-dependent deformation characteristics of the iliotibial tract. *J. Mech. Behav. Biomed. Mater.* **2012**, *16*, 81–86. [CrossRef]
28. Sichting, F.; Steinke, H.; Wagner, M.F.; Fritsch, S.; Hadrich, C.; Hammer, N. Quantification of material slippage in the iliotibial tract when applying the partial plastination clamping technique. *J. Mech. Behav. Biomed. Mater.* **2015**, *49*, 112–117. [CrossRef]
29. Zwirner, J.; Ondruschka, B.; Scholze, M.; Schulze-Tanzil, G.; Hammer, N. Mechanical properties of native and acellular temporal muscle fascia for surgical reconstruction and computational modelling purposes. *J. Mech. Behav. Biomed. Mater.* **2020**, *108*, 103833. [CrossRef]
30. Hammer, N.; Huster, D.; Fritsch, S.; Hadrich, C.; Koch, H.; Schmidt, P.; Sichting, F.; Wagner, M.F.; Boldt, A. Do cells contribute to tendon and ligament biomechanics? *PLoS ONE* **2014**, *9*, e105037. [CrossRef]
31. Giraldo-Gomez, D.M.; Leon-Mancilla, B.; Del Prado-Audelo, M.L.; Sotres-Vega, A.; Villalba-Caloca, J.; Garciadiego-Cazares, D.; Pina-Barba, M.C. Trypsin as enhancement in cyclical tracheal decellularization: Morphological and biophysical characterization. *Mater. Sci. Eng. C Mater. Biol. Appl.* **2016**, *59*, 930–937. [CrossRef]
32. Giraldo-Gomez, D.M.; Garcia-Lopez, S.J.; Tamay-de-Dios, L.; Sanchez-Sanchez, R.; Villalba-Caloca, J.; Sotres-Vega, A.; Del Prado-Audelo, M.L.; Gomez-Lizarraga, K.K.; Garciadiego-Cazares, D.; Pina-Barba, M.C. Fast cyclical-decellularized trachea as a natural 3D scaffold for organ engineering. *Mater. Sci. Eng. C Mater. Biol. Appl.* **2019**, *105*, 110142. [CrossRef] [PubMed]
33. Drumright, R.E.; Gruber, P.R.; Henton, D.E. Polylactic Acid Technology. *Adv. Mater.* **2000**, *12*, 1841–1846. [CrossRef]
34. Herod, T.W.; Chambers, N.C.; Veres, S.P. Collagen fibrils in functionally distinct tendons have differing structural responses to tendon rupture and fatigue loading. *Acta Biomater.* **2016**, *42*, 296–307. [CrossRef] [PubMed]